**Central European Journal of Energetic Materials**
ISSN 1733-7178; e-ISSN 2353-1843


*Cent. Eur. J. Energ. Mater.* 2020, *17*(2): 201-222; DOI 10.22211/cejem/124173
Article is available in PDF-format, in colour, at:
http://www.wydawnictwa.ipo.waw.pl/cejem/Vol-17-Number2-2020/CEJEM_01013.pdf


***Research paper***

# Experimental Investigation of the Effect of Polymers and Crystalline Qualities on the Safety Performance of LLM-105-based PBXs under Dynamic Compression and Shear

**Xiaogan Dai[1,#], Songwei He[1], Xiaona Huang[1,2,#], Zhijian Yang[1,*], Yushi Wen[1,**], Ming Li[1]**

[1] *Institute of Chemical Materials, China Academy of Engineering Physics, Mianyang 621900, Sichuan, China*
[2] *Department of Mechanical Engineering, City University of Hong Kong, 83 Tat Chee Avenue, Hong Kong*
[#] Dr. Xiaogan Dai and Ms. Xiaona Huang are both the first authors.
*E-mails:* * zhijianyang@caep.cn; ** wenys@caep.cn

**Abstract:** In recent years, the safety of ammunition has been an issue that has received close attention. The determination of the factors that influence the ignition of various 2,6-diamino-3,5-dinitropyrazine-1-oxide (LLM-105)-based polymer bonded explosives (PBXs) under external stimuli is of great importance for the development of safe PBX formulations. In order to further understand such factors and response characteristics, dynamic compression and shear tests on PBXs containing fluorinated rubber, 1,1-diamino-2,2-dinitroethene (FOX-7), polyethylene wax (PEW), and high quality or rough LLM-105 were conducted. A high speed camera, SEM, and XPS imaging were used to examine the recovered samples, variations in the structures of LLM-105 based-PBXs, and the surface chemical composition after compression and shear. For a given sample the ignition threshold in a shear test was generally lower than that in a compression test. We have also determined the factors causing decomposition. The ignition mechanism under dynamic compression and shear were helpful for developing better PBX formulations.

**Keywords:** compression ignition, shear ignition, effect mechanism, LLM-105-based PBXs

## 1 Introduction

The safety of ammunition has received much attention in recent years. Developing polymer bonded explosives (PBXs), with a focus on safety, has been a major trend in this area [1-7]. The safety of a PBX is typically evaluated using mechanical sensitivity tests and large-scale safety tests [1], since its mechanical properties are critical to hot spot formation and impact sensitivity [8]. The sample sizes used in mechanical sensitivity tests range from 30 to 50 mg [2-5]; these values are smaller than the amount of explosive used in a real case, thus mechanical sensitivities are unsuitable for evaluating safety. The sample sizes are above 200 g in large scale tests, such as Bullet Impact, Susan, or Cook off tests [6, 7], and these tests are very expensive and difficult to conduct. In order to reduce cost, decrease testing time, and simplify the test procedures, moderate scale safety tests can be conducted with 3 g samples that are 20×5 mm (diameter × thickness), whose masses are around 100 times those used in mechanical sensitivity tests. The samples for moderate scale tests are closer in size and mass to real explosive charges. The moderate scale tests improve the comparability of experiments and effectively reduce experimental costs. Moderate scale safety tests like dynamic compression and shear tests can facilitate efficient selection of PBX formulations.

Ignition is usually induced by impact compression or impact shear in large scale safety tests, such as the Spigot, Bullet Impact, and Susan tests [9-11]. Compression and shear tests are the primary focus in moderate scale tests. Dynamic compression and shear tests are helpful for better understanding the ignition mechanism in Spigot, Bullet Impact, and Susan tests, where compression and shear are combined. These two methods were applied to a 2,6-diamino-3,5-dinitropyrazine-1-oxide (LLM-105)-based PBX, a potential explosive [12, 13]. With a density of 1.9097 ±0.0005 g/cm$^3$ at ambient temperature, LLM-105 has great performance from various aspects, as has been indicated by a numbers of researchers, *e.g.* it releases 15% more energy than 2,4,6-triamino-1,3,5-trinitrobenzene (TATB). Mechanical sensitivity tests show that this material is quite safe (*i.e.* insensitive to impact, spark, friction, shockwave, and heat); the DSC heat release peak temperature (354 °C) is almost as high as that for TATB. Although some previous publications [14] have reported an insensitive booster explosive based on LLM-105 [15], a deeper understanding of the safety of an LLM-105-based PBX is still required [16]. For example, the

polymeric components, crystal quality, and shape greatly affect the sensitivity of LLM-105-based PBXs, while the main safety factors and ignition mechanism under compression and shear are still unclear. These are all very important for developing safe PBX formulations. We also need to know what kind of additives improve safety during compression and shear.

This paper is organized as follows. The experimental methods and diagnosis techniques are briefly introduced in Section 2, the experimental results and discussion are presented in Section 3, and Section 4 draws together the conclusions.

## 2 Experiment Design

Dynamic compression and shear tests were designed. 20×5 mm (diameter × thickness) samples were used in both cases. The original materials were placed in a high speed rotating machine to form granules, which were then compressed into explosive cylinders.

### 2.1 Dynamic compression tests

The apparatus for the compression tests is shown in Figures 1 and 2. The explosive sample was confined in a polyethylene ring in a compression device. The hammer was lifted to a preset height and released. The hammer fell and collided with the impact pillar in the compression device. The sample can then react in a confined impact compression scenario. This impact test is similar to the confined impact test reported previously [17].


(a) (b)

**Figure 1.** Scheme (a) and photograph (b) of a small scale impact compression test

As shown in Figure 2, the test device consists of impact pillar, explosive sample, steel sleeve, polyethylene ring, 1 mm steel flake, PVDF pressure gauge, and steel base. The hammer was designed with a 50 kg mass and its drop height ($H$) ranged from 0.25 to 12 m.

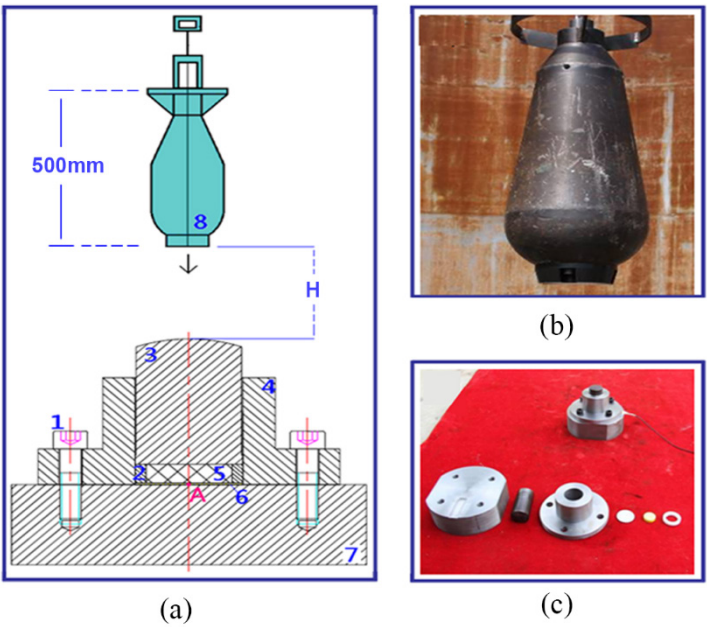


**Figure 2.** Compression test apparatus: (a) scheme: 1 – bolt, 2 – polyethylene ring, 3 – impact pillar, 4 – steel sleeve, 5 – explosive samples, 6 – steel flake, 7 – steel base, 8 – 50 kg hammer, and A – PVDF pressure gauge, (b) hammer, and (c) impact device

The response of an LLM-105-based PBX to dynamic compression was observed with a high speed camera, air shockwave overpressure gauges, and impact pressure gauges. The impact process and the impact posture of the hammer were recorded with a high speed camera at 10000 fps. The reaction overpressure from the sample was obtained with two air shockwave overpressure gauges. Each gauge was set 1 m away and 0.5 m above the impact point. The pressure at the explosive impact surface was measured with an embedded PVDF pressure gauge, which was placed on the back of the steel flake under the explosive sample, denoted as point A in Figure 2. A scanning electron microscope (SEM) and X-ray photoelectron spectroscopy (XPS) were used to examine the examples after testing.

## 2.2 Shear test

A schematic diagram of the shear test apparatus is shown in Figure 3. An explosive sample was embedded in the shear device. The hammer was lifted to a preset height and released. The hammer fell and collided the impact pillar of the shear device. The sample can then react in a confined shear scenario.

A photograph of the equipment used for the shear tests is also shown in Figure 3. The shear test device is similar to the compression device, but the structure was modified to ensure that a shear stress was applied to the sample. The hammer used in the shear tests was the same as that used in the compression tests.

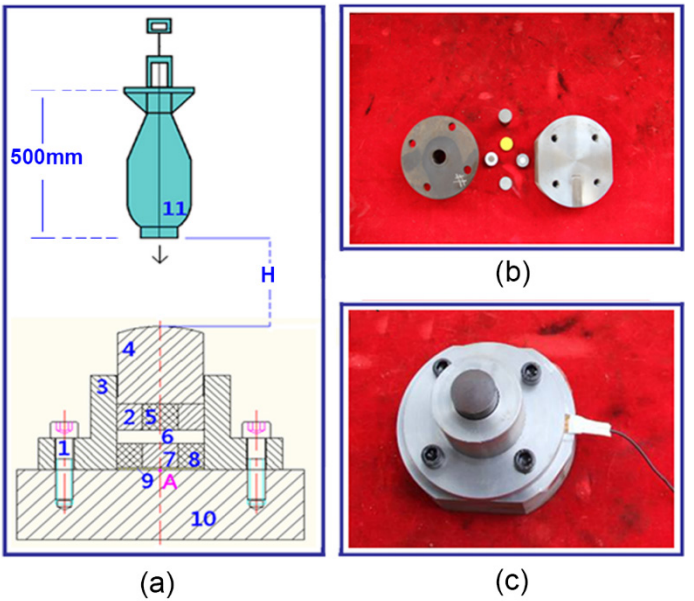


**Figure 3.** Shear test apparatus: (a) scheme: 1 – bolt, 2 – steel ring, 3 – steel sleeve, 4 – impact pillar, 5 – polyethylene pillar, 6 – explosive sample, 7 – steel pillar, 8 – polyethylene ring, 9 – steel flake, 10 – steel base, 11 – 50 kg hammer and A – PVDF pressure gauge, (b, c) shear device

The response to the shear tests was observed with a high speed camera, air shockwave overpressure gauges, PVDF pressure gauges, SEM and XPS equipment.

### 2.3 Explosive samples

A series of experiments was performed with several LLM-105-based PBX formulations (PEW denotes polyethylene wax), as follows:

– LLM-A: LLM-105/FOX-7/F-rubber/PEW = 80/15/4/1,
– LLM-B: LLM-105/F-rubber/desensitizing polymers = 95/2/3,
– LLM-C: LLM-105/FOX-7/F-rubber = 35/60/5,
– LLM-H: LLM-105 (high quality)/F-rubber = 95/5,
– LLM-R: LLM-105 (rough quality)/F-rubber = 95/5.

The LLM-105 crystals used in this work were from a single batch with an average particle size of 60 μm.

## 3 Results and Discussion

### 3.1 Compression test results

#### *3.1.1 High speed camera imaging*

Figure 4 shows typical high speed camera images of PBXs during the compression tests. LLM-A and LLM-C explosives reacted after impact when the hammer was dropped from 3.0 m, releasing a lot of gas. As a result, the impact pillar was ejected and the hammer rebounded. For LLM-R, gas was ejected after impact when the hammer was dropped from 4.0 m, indicating a GO result (result of reaction or ignition). For LLM-H, a lot of gas and yellow powder were released after impact when the hammer was dropped from 6.0 m, indicating a GO result. The high speed camera pictures are not shown for this example.

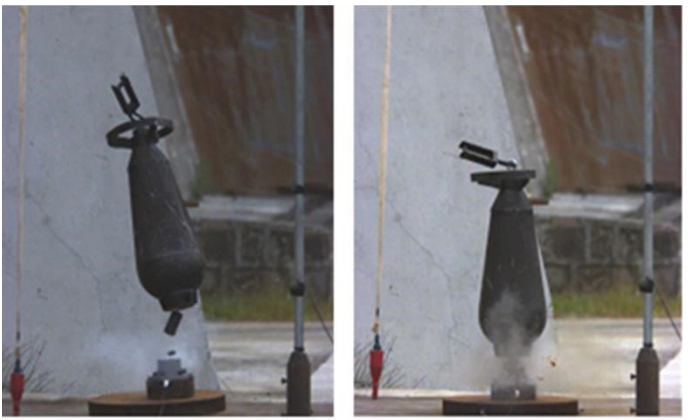


**Figure 4.** Typical images from the high speed camera during compression tests of LLM-105-based PBXs when impacted from 3.0 m: (a) LLM-A and (b) LLM-C

### *3.1.2 Recovered debris*

Photographs of the recovered debris from LLM-105-based PBXs and the confinement equipment after the compression tests are shown in Figure 5. LLM-A exhibited a carbonized darkened surface on the tablet when the hammer was dropped from 2.0 m, and the explosive surface became cracked when the hammer was dropped from 3.0 m. The LLM-B samples were compressed and cracked at the edges when the hammer was dropped from 3.0 and 4.0 m; the surfaces of the samples and the steel flakes were blackened, indicating slight decomposition. LLM-C exhibited cracks on the surface of the tablet when the hammer was dropped from 2.0 m. The surface cracked into pieces and obviously reacted when the hammer was dropped from 3.0 m. LLM-H exhibited penetrating cracks on the surface of the tablet when the hammer was dropped from 3.0 m, the tablet cracked due to delamination at 4.0 m, and no sample was recovered at 6.0 m; a carbonized darkened surface can be seen on the surface of the device. LLM-R did not exhibit cracks on the surface of the tablet when the hammer was dropped from 3.0 m, while the tablet cracked due to delamination when the hammer was dropped from 4.0 m. Plenty of sample material was recovered, and a carbonized darkened surface can be seen on the surface of the device.

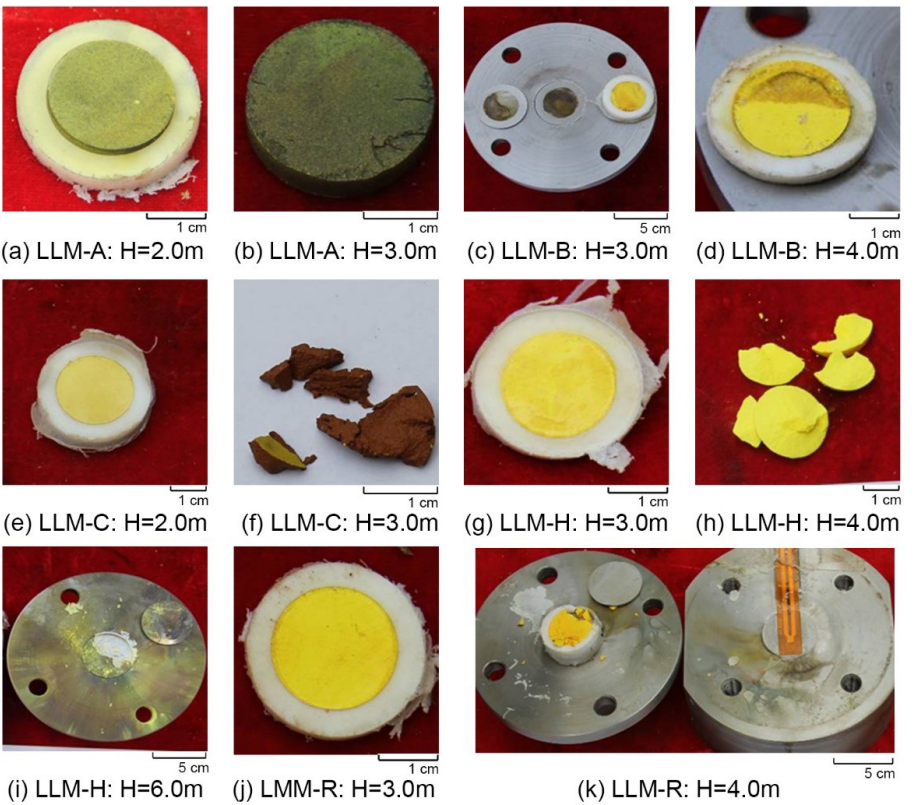


**Figure 5.** Photographs of recovered debris from LLM-105-based PBXs and their confinement equipment after compression tests

Figure 5 shows the discoloration in LLM-A and LLM-C, both of which contain FOX-7. This discoloration is not found with LLM-B, -R or -H samples, which do not contain FOX-7. The discoloration is probably due to the presence of FOX-7. FOX 7 has an α→β phase transition around 120 °C [18]. The crystal volume changes significantly when the crystal passes through this transition, which would account for some of the cracks observed in these samples if the impact produces sufficient heating due to friction.

### *3.1.3 Pressure measurements*

Typical pressure *vs.* time curves at point A during the compression tests are shown in Figure 6. The peak value with LLM-A was approximately 1.15 GPa when the hammer was dropped from 2.0 m, with a duration of approximately 2.0 ms. The peak value was approximately 1.61 GPa when the hammer was dropped from 3.0 m.

The peak value with LLM-B was approximately 1.24 GPa when the hammer was dropped from 3.0 m, with a duration of approximately 1.3 ms. The peak value with LLM-C was about 1.5 GPa when the hammer was dropped from 3.0 m.

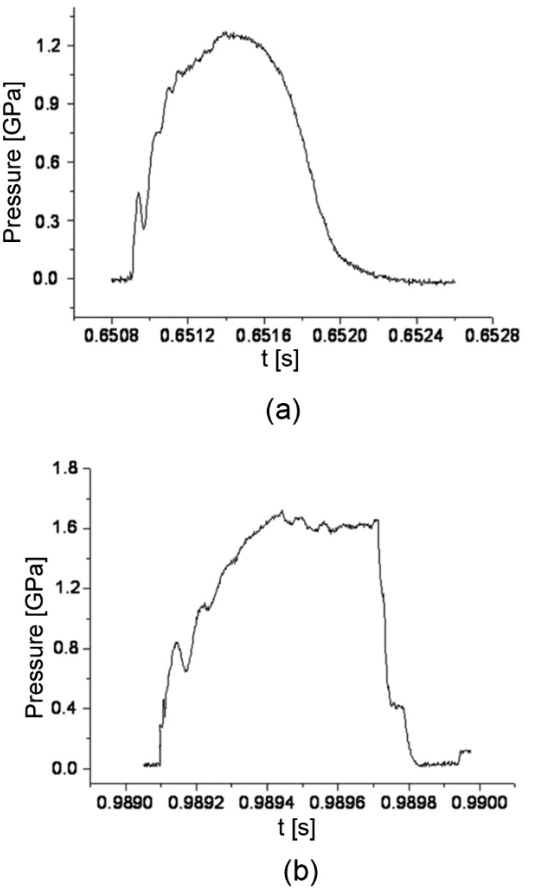


**Figure 6.** Typical pressure curves at point A for LLM-105-based PBXs in compression tests: LLM-B (a) and LLM-C (b), both for $H = 3.0$ m

According to the pressure histories, the high speed camera images, and the photographs of the debris, details of the compression test results can be drawn and are listed in Table 1, including pressure peaks, duration, and reaction results (GO or NO GO). LLM-A reacted when the pressure reached 1.15 GPa during the compression test. The ignition pressure threshold of LLM-B was 1.24 GPa. The ignition threshold of LLM-B ranged from 1.28 to 1.54 GPa, while the threshold of LLM-R ranged from 1.35 to 1.46 GPa.

**Table 1.** Compress test results for various PBX formulations

| Sample | Drop height [m] | Peak pressure [GPa] | Pulse width [ms] | Reaction result |
|---|---|---|---|---|
| LLM-A | 2.0 | 1.15 | 2.0 | GO |
| | 3.0 | 1.61 | 3.0 | GO |
| LLM-B | 3.0 | 1.24 | 1.3 | GO |
| | 4.0 | 1.48 | 2.0 | GO |
| LLM-C | 3.0 | 1.50 | – | GO |
| LLM-H | 3.0 | 1.28 | 1.4 | NO GO |
| | 6.0 | 1.54 | – | GO |
| LLM-R | 3.0 | 1.35 | 1.3 | NO GO |
| | 4.0 | 1.46 | 1.9 | GO |

### *3.1.4 Results analysis*

Table 2 shows a subset of the relevant shockwave overpressure, the ignition drop height threshold, and the reaction results from the experimental data. The compression tests all resulted in decomposition and burning. The drop height ignition threshold for high quality LLM-105-based PBX (LLM-H) was higher than that of rough LLM-105-based PBX (LLM-R).

**Table 2.** Shockwave overpressure, ignition drop height threshold, and reaction degree from compression tests

| Sample | Overpressure | Ignition threshold [m] | Reaction result |
|---|---|---|---|
| LLM-A | not recorded | <2 | Decomposition/burning |
| LLM-B | | <3 | Decomposition |
| LLM-C | | 2~3 | Decomposition/burning |
| LLM-H | | 4~6 | Decomposition/burning |
| LLM-R | | 3~4 | Decomposition/burning |

## 3.2 Shear test results

### *3.2.1 High speed camera imaging*

Figure 7 shows typical high speed camera results from the shear tests. A lot of gas and yellow powder were released from LLM-A after shear when the hammer was dropped from 0.5 m, indicating a GO result. LLM-C exhibited similar results when the hammer was dropped from 1.0 m, indicating a GO result. A lot of gas was released from LLM-B after shear when the hammer was dropped from 1.0 m, causing the impact pillar to eject and the hammer to rebound due

to the gas pressure, indicating a GO result. For LLM-R and LLM-H, the results were similar to those obtained with LLM-B when the hammer was dropped from 1.0 and 0.5 m, respectively, indicating a GO result.

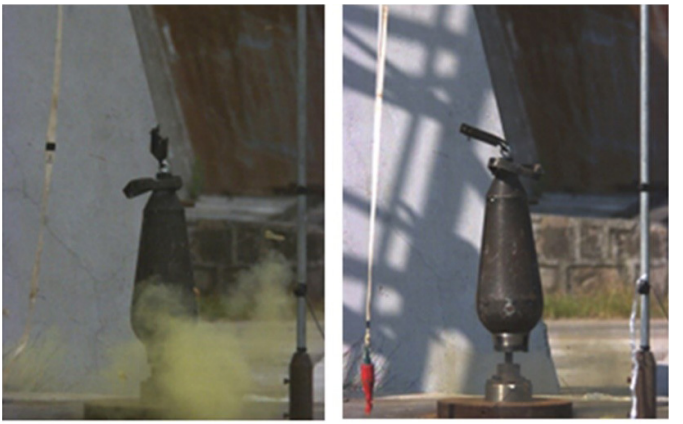


**Figure 7.** Typical high speed camera pictures of shear tests of LLM-105-based PBXs: (a) LLM-A (0.5 m) and (b) LLM-B (1.0 m)

### *3.2.2 Recovered debris*

Photographs of the recovered debris after the shear tests are shown in Figure 8. LLM-A exhibited obvious cracks and concaves on the surface of the tablet when the hammer was dropped from 0.25 m; the sample cracked into pieces and obvious signs of reaction appeared on the surface of the device when the hammer was dropped from 0.5 m, and the sample was partially recovered. For LLM-B there were no obvious cracks in the tablet when the hammer was dropped from 0.5 m; none of the sample was recovered when the hammer was dropped from 1.0 m, and there were obvious signs of reaction on the device. The sample cracked into pieces and a blackened surface were observed on the device when the hammer was dropped from 2.0 m.

LLM-C exhibited obvious cracks and concaves on the surface of the tablet when the hammer was dropped from 0.5 m; the sample cracked into pieces and obvious signs of reaction can be seen on the device when the hammer was dropped from 1.0 m, and the sample was partially recovered. LLM-H exhibited obvious concaves on the tablet when the hammer was dropped from 0.25 m; no sample was recovered at 0.5 m, and obvious signs of reaction were seen on the device. The sample cracked into pieces and obvious signs of reaction were seen on the device when the hammer was dropped from 2.0 m,

and the sample was partially recovered. LLM-R did not exhibit cracks or concaves on the surface of the tablet when the hammer was dropped from 0.5 m; no sample was recovered at 1.0 m drop height; the sample cracked into pieces and obvious signs of reaction were observed on the device when the hammer was dropped from 2.0 and 3.0 m, and the sample was partially recovered.

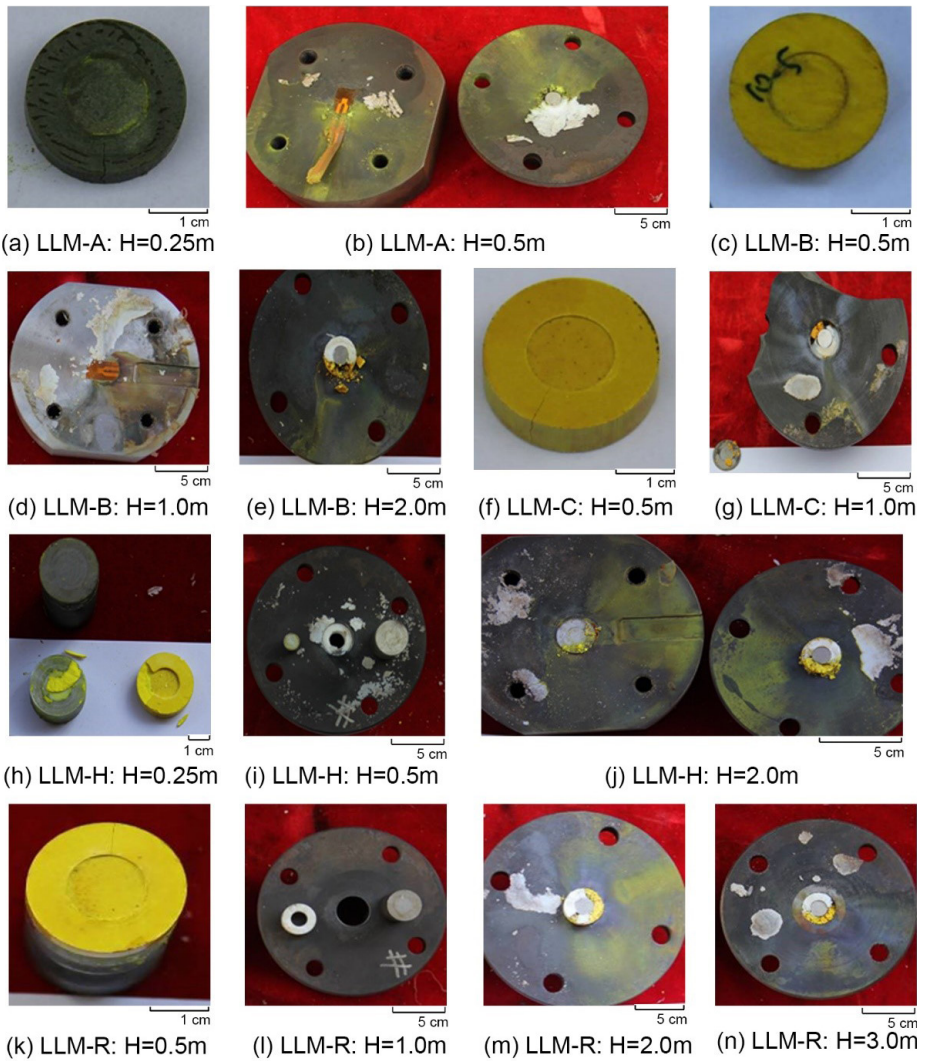


**Figure 8.** Photographs of recovered debris of LLM-105-based PBXs and confinement equipment after shear tests

### *3.2.3 Pressure measurements*

Typical pressure *vs.* time curves at point A during the shear tests are shown in Figure 9. The peak value from LLM-A was approximately 0.7 GPa when the hammer was dropped from 0.5 m, with a duration of approximately 1.5 ms. The peak value from LLM-B was approximately 1.27 GPa when the hammer was dropped from 2.0 m, with a duration of approximately 1.2 ms.

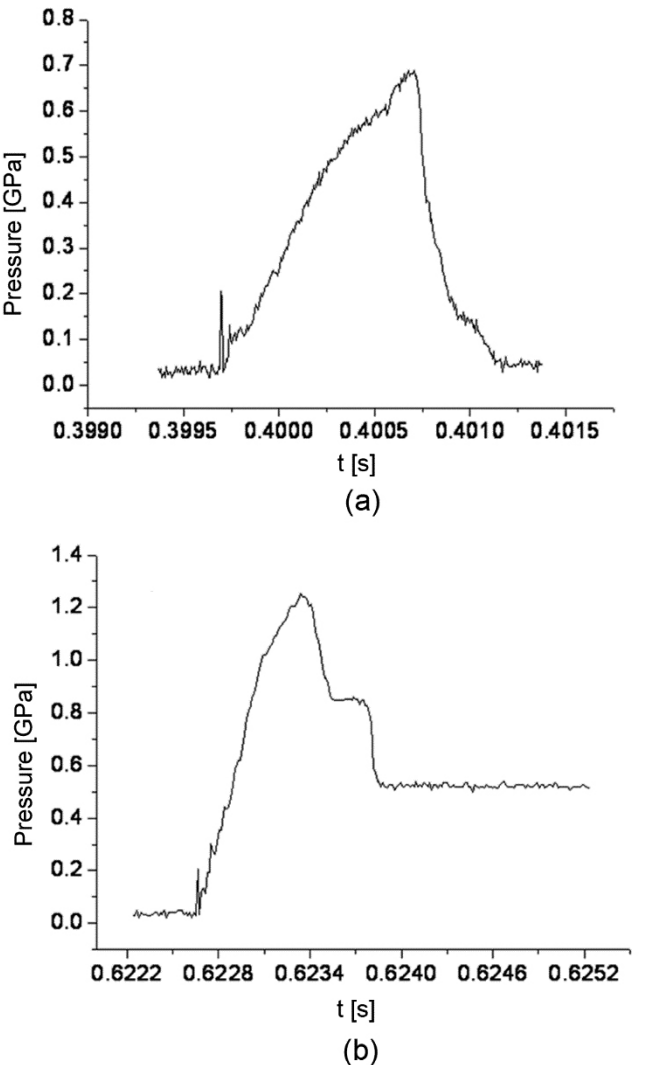


**Figure 9.** Typical pressure curves of LLM-105-based PBXs during shear tests at point A, for LLM-A at H = 0.5 m (a) and LLM-B at H = 2.0 m (b)

Details of the shear tests are listed in Table 3, including drop height, peak pressure, duration and reaction results. The ignition pressure thresholds for LLM-A, LLM-H, LLM-C, LLM-B, and LLM-R ranged from 0.57 to 0.69, 0.91 to 0.99, 0.90 to 1.25, 0.98 to 1.25, and 1.0 to 1.28 GPa, respectively. A higher ignition pressure threshold indicates a safer formulation under shear stimulus.

**Table 3.** Pressure at point A during shear tests

| Sample | Drop height [m] | Peak pressure [GPa] | Pulse width [ms] | Reaction results |
|---|---|---|---|---|
| LLM-A | 0.25 | 0.57 | 2.6 | NO GO |
| | 0.5 | 0.69 | – | GO |
| LLM-B | 0.5 | 0.98 | 2.86 | NO GO |
| | 2.0 | 1.25 | – | GO |
| LLM-C | 0.5 | 0.9 | – | NO GO |
| | 1.0 | 1.25 | – | GO |
| LLM-H | 0.25 | 0.91 | 3.6 | NO GO |
| | 0.5 | 0.99 | – | GO |
| | 1.0 | 1.1 | – | GO |
| | 2.0 | 1.39 | – | GO |
| LLM-R | 0.5 | 1.0 | 2.66 | NO GO |
| | 1.0 | 1.28 | – | GO |
| | 2.0 | 1.4 | – | GO |

### *3.2.4 Results analysis*

Table 4 shows a subset of the shockwave overpressure, the drop height, and the reaction results according to the experimental shear test data. The highest reaction degree for these formulations was deflagration. The drop height ignition threshold of high quality LLM-105-based PBX (LLM-H) was lower than that of rough quality LLM-105-based PBX (LLM-R). Generally, the samples were much easier to react under shear than under compression.

**Table 4.** Shockwave overpressure and reaction results from shear tests

| Sample | Drop height [m] | Shockwave overpressure [kPa] | Reaction results |
|---|---|---|---|
| LLM-A | 0.25 | Not recorded | No reaction |
| | 0.5 | | Decomposition/burning |
| LLM-B | 0.5 | Not recorded | No reaction |
| | 1.0 | | Decomposition/burning |
| | 20 | 7 | Deflagration |
| LLM-C | 0.5 | Not recorded | No reaction |
| | 1.0 | | Decomposition/burning |
| LLM-H | 0.25 | Not recorded | No reaction |
| | 0.5 | | Decomposition/burning |
| | 1.0 | 4.3 | Deflagration |
| | 2.0 | 7 | Deflagration |
| LLM-R | 0.5 | Not recorded | No reaction |
| | 1.0 | | Decomposition/burning |
| | 2.0 | | Decomposition/burning |
| | 3.0 | 4.5 | Deflagration |

## 3.3 Safety of LLM-105-based PBX formulations

### *3.3.1 The influence of crystal quality on PBX safety*

The drop height and pressure ignition thresholds for these formulations are shown in Table 5. The only difference between formulations LLM-A and LLM-C is the presence of PEW. Table 5 shows that using PEW can remarkably reduce the safety of LLM-105-based PBXs, which may be due to the hardness of PEW.

In compression tests, the drop height ignition threshold for high quality LLM-105-based PBX (LLM-H) was higher than that of the rough quality PBX (LLM-R). In shear tests, the drop height ignition threshold of LLM-H was lower than that of LLM-R, which differs from HMX-based PBXs. The Young›s modulus of LLM-H (~2.5 GPa) was higher than that of LLM-R (~2.0 GPa). A higher Young's modulus may lead to higher shear resistance and more energy localization, thus higher quality LLM-105-based PBXs would be easier to ignite, according to a previous shear ignition study [19, 20].

**Table 5.** Drop height and pressure ignition thresholds for several LLM-105 based PBXs

| Sample | Shear ignition threshold | | Compression ignition threshold | |
|---|---|---|---|---|
| | Drop height [m] | Pressure [GPa] | Drop height [m] | Pressure [GPa] |
| LLM-B | 0.5~1.0 | 0.98~1.25 | <3.0 | <1.24 |
| LLM-C | 0.5~1.0 | 0.9~1.25 | 2.0~3.0 | – |
| LLM-A | 0.25~0.5 | 0.57~0.69 | <2.0 | <1.15 |
| LLM-H | 0.25~0.5 | 0.91~0.99 | 4.0~6.0 | 1.28~1.54 |
| LLM-R | 0.5~1.0 | 1.0~1.28 | 3.0~4.0 | 1.35~1.46 |

SEM images of the rough quality and high quality LLM-105 crystals are shown in Figure 10. The granule morphology of the high quality LLM-105 crystals is more regular, smoother, has sharper edges, and has less broken and mixed crystals, than the rough quality LLM-105 crystals.

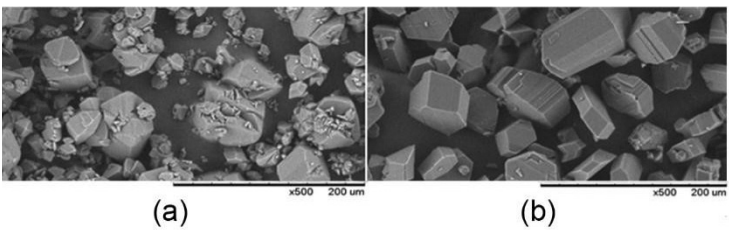


**Figure 10.** SEM images of rough quality (a) and high quality (b) LLM-105 crystals (the average particle size of the crystals was about 60 μm)

The ignition mechanism during shear tests is obviously different from that in compression tests, and the granule morphologies of high and rough quality LLM-105 crystals are quite different. As a result, the response of the different crystals differ in the compression and shear tests. The effect of the crystal quality of LLM-105 on shear safety requires further study.

### *3.3.2 Surface structure of LLM-105-based PBXs*

SEM images of LLM-A, LLM-C, and LLM-R samples recovered after the compression tests are shown in Figure 11. Tiny holes generated on the surface of the samples remained after the GO tests, resulting from reaction and vaporization. No obvious changes were observed on the surface of the samples remaining after NO GO tests.

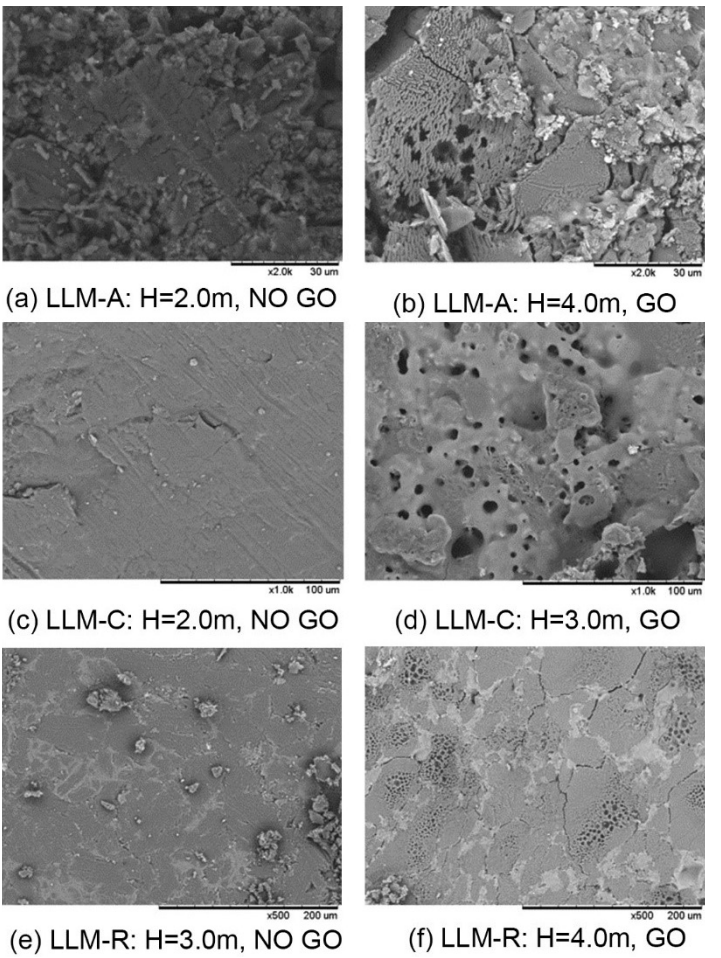


**Figure 11.** SEM images of several LLM-105-based PBXs recovered from compression tests

SEM images of LLM-B, LLM-C, LLM-H, and LLM-R samples recovered after the shear tests are shown in Figure 12. Tiny holes appeared on the surface of samples remaining after the GO tests, resulting from reaction and vaporization. Obvious marks due to shear and friction were observed on the surfaces of the LLM-B and LLM-C NO GO samples, resulting in striped surfaces. No obvious changes can be seen on the surfaces of the LLM-R and LLM-H NO GO samples.

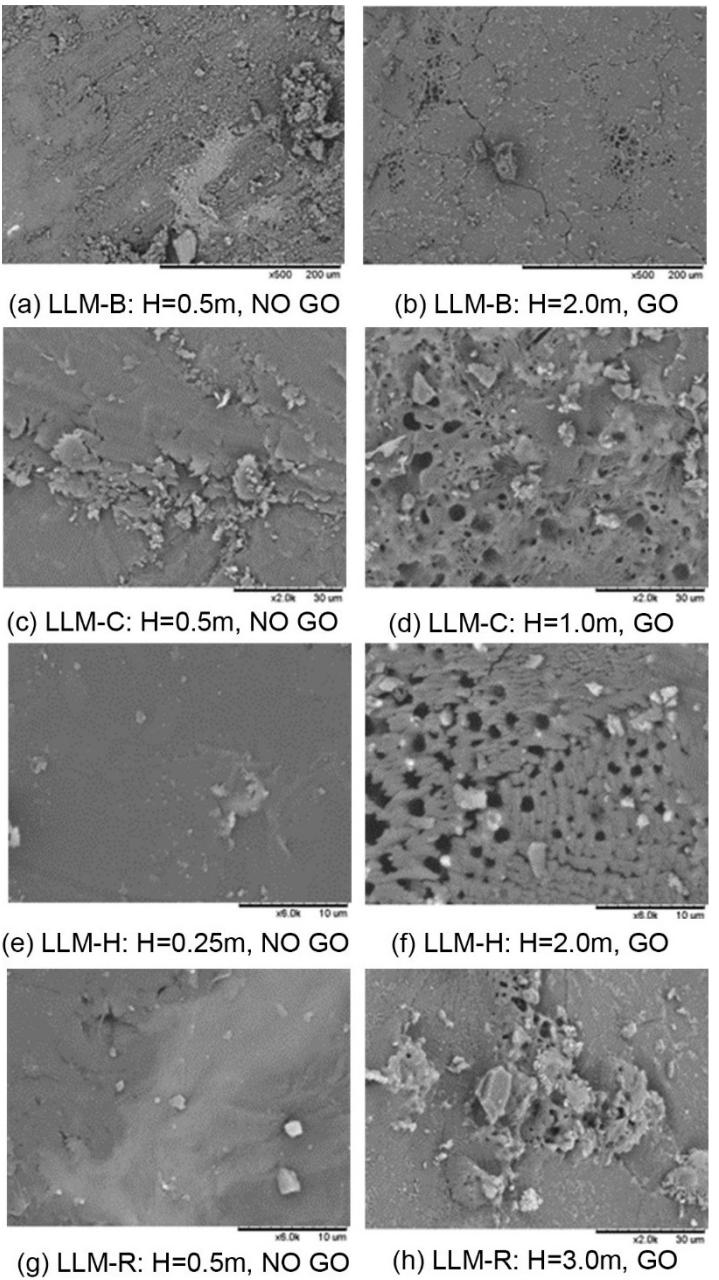


**Figure 12.** SEM images of several LLM-105-based PBXs recovered from shear tests

### *3.3.3 Elemental analysis after testing*

XPS was used to analyze the chemical composition of the sample surfaces after impact or shear. Changes in the chemical composition provide evidence of reaction. C, H, O, N, and F are the main elements in these samples, where C, H, O and N come primarily from LLM-105, while F comes mainly from the fluorinated rubber polymer. The C, H, O and N contents normally decrease after an impact-induced reaction or vaporization. The F content usually increases in low violence reactions without growth, because fluorine containing rubber does not participate in the ignition. Here, we paid close attention to the F content, considering it to be evidence of ignition. LLM-A, LLM-B, and LLM-C samples were tested and the elemental changes between before and after testing are shown in Figure 13.

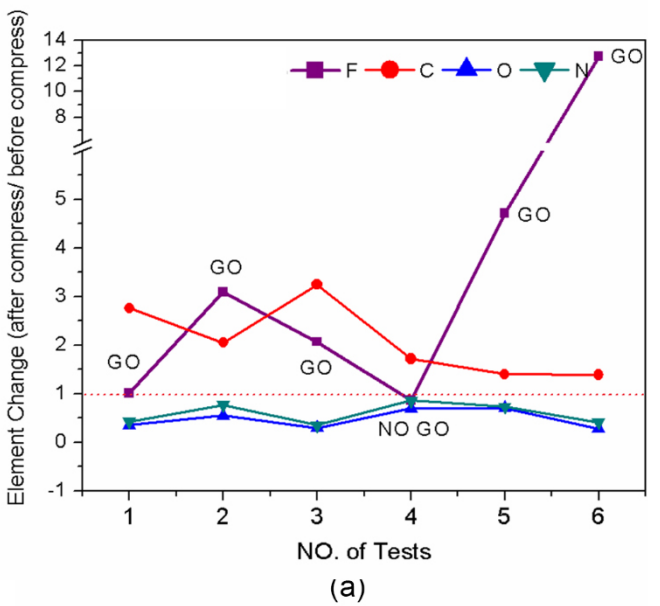

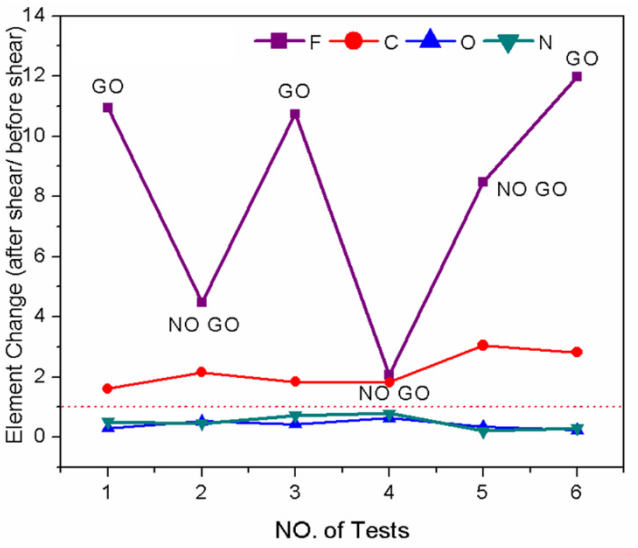


(b)

**Figure 13.** Changes in F, C, O, and N content (%) of samples, LLM-A, LLM-B and LLM-C, before and after typical testing rounds (points above the red dashed line (Y = 1) indicate increased elemental content) in compressed tests (a) and shear tests (b)

Figure 13 shows that the elemental content (%) had usually changed after testing. On the whole, the F and C contents had increased (points above the line Y = 1) and the contents of N and O had decreased (points below the line Y = 1). The F content had decreased after one test (NO GO) and increased after 5 subsequent tests (GO), as shown in Figure 13(a). Similarly, the F content had decreased after 3 tests (NO GO), and increased after 3 subsequent tests (GO), as shown in Figure 13(b). There in a definite relationship between the F content at the surface of the recovered samples and whether or not they had ignited. Generally, the F content will increase after a test with a GO result. No similar trend could be found for the remaining elements investigated here.

## 4 Conclusions

Compression and shear tests combined with SEM and XPS analysis were used to examine rough LLM-105-based PBXs in order to better understand their safety response characteristics. The results showed that compression and shear tests

have different effects on high quality and rough LLM-105-based PBXs. The ignition threshold in a shear test is generally lower than that in a compression test for a given sample. The ignition mechanism corresponding to the two loading methods may be different; for the present this is still insufficiently clear. Each evaluation method can effectively assess the corresponding sensitivity.

The use of polymers like PEW can increase the sensitivity to compression and shear. The impact safety of LLM-105-based PBXs can be improved by using high quality LLM-105 crystals instead of rough quality crystals, while the impact-shear safety of these PBXs will be worse after such a replacement. An interesting discoloration in the PBXs containing FOX-7 was observed, which is probably due to the crystal-crystal phase transition of FOX-7 near 120 °C. Furthermore, the XPS results show that the F content will generally increase after a test with a GO result.

## Acknowledgments

The authors greatly appreciate financial support from the National Natural Science Foundation of China (11972329, 11702266, 51703211, and 11504153).

## References

[1] Teipel, U. *Energetic Materials: Particle Processing and Characterization*. John Wiley & Sons, Hoboken, New Jersey, **2006**, pp. 8; ISBN 3-527-30240-9.
[2] Leiber, C.O. *Assessment of Safety and Risk with a Microscopic Model of Detonation*. Elsevier, Amsterdam, **2003**, pp. 163-175; ISBN 0-444-51332-9.
[3] Dubovik, A.V.; Matveev, A.A. Explosion-like Reactions in Poly(vinyl chloride) on Impact. *Dokl. Phys. Chem*. **2012**, *446*(2): 163-165.
[4] Field, J.E.; Walley, T.M.; Proud, W.G.; Goldrein, H.T.; Siviour, C.R. Review of Experimental Techniques for High Rate Deformation and Shock Studies. *Int. J. Impact Eng*. **2004**, *30*(7): 725–775.
[5] Swallowe, G.M.; Field, J.E. Effect of Polymers on the Drop-Weight Sensitiveness of Explosives. *Int. Det. Symp., Proc., 7th*, Annapolis, MD, USA, **1981**, 24.
[6] Dai, X.; Han, D.; Xiang, Y.; Li, T. The Measurement and Numerical Simulation of the Projectile Deformation in Susan Test. *Chin. J. Energ. Mater*. **2004**. *12*(4): 235-238.
[7] Dai, X.; Shen, C.; Lü, Z.; Xiang, Y. Reaction Properties for Different Size PBX-2 Explosives in Bullet Impact Test. *Chin. J. Energ. Mater*. *(HanNeng CaiLiao)* **2008**, *16*(4): 432-435.
[8] Hu, Z.; Luo, H.; Bardenhagen, S.G.; Siviour, C.R.; Armstrong, R.W.; Lu, H. Internal Deformation Measurement of Polymer Bonded Sugar in Compression by Digital Volume Correlation of *in-situ* Tomography. *Exp. Mech.* **2015**, *55*(1): 289-300.

[9] Ma, D.; Chen, P.; Zhou, Q.; Dai, K. Ignition Criterion and Safety Prediction of Explosives under Low Velocity Impact. *J. Appl. Phys.* **2013**, *114*(11): 113505.
[10] Dai, X.; Shen, C.; Wen, Y.; Xiang, Y. Reaction Rule for Explosive under Different Shape Warhead Impact in Steven Test. *Chin. J. Energ. Mater*. *(HanNeng CaiLiao)* **2009**, *17*(1): 50-54.
[11] Dai, X.; Wen, Y.; Huang, H.; Zhang, P.; Wen, M. Impact Response Characteristics of a Cyclotetramethylene Tetranitramine Based Polymer-bonded Explosives under Different Temperatures. *J. Appl. Phys*. **2013**, *114*(11): 114906.
[12] Tran, T.D.; Pagoria, P.F.; Hoffman, D.M.; Cutting, J.L.; Lee, R.S.; Simpson, R.L. *Characterization of 2,6-Diamino-3,5-Dinitropyrazine-1-Oxide (LLM-105) as an Insensitive High Explosive Material*. LLNL Report UCRL-JL-147932, **2002**.
[13] Hoffman, D.M.; Lorenz, K.T.; Cunningham, B.; Gagliardi, F. *Formulation and Mechanical Properties of LLM-105 PBXs*. LLNL Report LLNL-CONF-402822, **2008**.
[14] Tran, T.D.; Pagoria, P.F.; Hoffman, D.M.; Cunningham, B.; Simpson, R.L.; Lee, R.S. Cutting, J.L. Small-scale Safety and Performance Characterization of New Plastic Bonded Explosives Containing LLM-105. *Int. Det. Symp., Proc., 12th,* San Diego, CA, **2002**, 440.
[15] Xu, W.; An, C.; Wang, J.; Dong, J.; Geng, X. Preparation and Properties of an Insensitive Booster Explosive Based on LLM-105. *Propellants, Explos. Pyrotech*. **2013**, *38*(1): 136-141
[16] Zhang, C.; Zhang, X.; Ma, L.; Wang, Y.; Chen, J.; Yuan, Z.; Yang, L.; Zhou, R. The New Progress of 2,6-Diamino-3,5-dinitro Pyrazine-1-oxide. *Sci. Technol. Eng.* **2015**, *15* (23): 1.
[17] Dai, X.; Huang, Q.; Huang, F.; Li, M.; Wen, Y.; Liu, X. The Development of a Confined Impact Test for Evaluating the Safety of Polymer-bonded Explosives during Warhead Penetration. *Propellants, Explos. Pyrotech.* **2015**, *40*(5): 665-673
[18] Evers, J.; Klapötke, T.M.; Mayer, P.; Oehlinger, G.; Welch, J. α- and β-FOX-7, Polymorphs of a High Energy Density Material, Studied by X-ray Single Crystal and Powder Investigations in the Temperature Range from 200 to 423 K. *Inorg. Chem.* **2006**, *45*(13): 4996-5007.
[19] Xue, X.; Wen, Y.; Long, X.; Li, J.; Huang, H.; Zhang, C. Influence of Dislocations on the Shock Sensitivity of RDX: Molecular Dynamic Simulations by Reactive Force Field. *J. Phys. Chem. C* **2015**, *119*(24):13735.
[20] Liu, R.; Chen, P.W.; Zhang, X.T.; Zhu, S.P. Non-Shock Ignition Probability of Octahydro-1,3,5,7-tetranitrotetrazocine-based Polymer Bonded Explosives Based on Microcrack Stochastic Distribution. *Propellants, Explos. Pyrotech.* **2020**, *45*(4): 568-580.

Received: October 24, 2018
Revised: June 18, 2020
First published online: June 25, 2020